A Higher-Order Method For Finding Vortex Core Lines

Martin Roth and Ronald Peikert

Swiss Center for Scientific Computing,   ETH Zürich,   Switzerland
roth@acm.org,   peikert@scsc.ethz.ch

Abstract

This paper presents a novel method to extract vortical structures from 3D CFD vector fields automatically. It discusses the underlying theory and some aspects of the implementation. Making use of higher-order derivatives, the method is able to locate bent vortices. In order to structure the recognition procedure, we distinguish locating the core line from calculating attributes of strength and quality. Results are presented on several flow fields from the field of turbomachinery.

Keywords: vortex cores, 3D vector fields, CFD analysis, feature extraction, feature-based visualization

1 Introduction

In spite of recent advances, visualizing complex flow fields remains a major challenge. For 2D domains, texturing techniques ([3], [22], [13]) have been very successful in displaying a vector field in its entirety. Texture methods can also be applied in 3D ([4], [8]). However, such a direct mapping of the entire field to graphical objects can not successfully convey all information present in a spatially complex flow field. Visualization of 3D flows is therefore highly selective. Classical visualization techniques require careful and laborious selection of streamlines or isosurface levels to display the essential properties of a flow. Recent methods ([20], [21]) aim at assisted or automatic selection and display of essential flow features, leading to the field of feature-based visualization, which integrates data analysis and recognition techniques as first steps into the visualization pipeline.

Helman and Hesselink [6] introduced the topology of a vector field as such an automatic feature-based visualization technique. This work has recently been extended to symmetric tensor fields [12] and second-order singularities [17]. Other efforts have concentrated on tracking coherent structures in large time-varying flows ([24], [20]).

Turbomachinery flows

Our field of application, CFD simulations of hydraulic turbomachinery [11], is particularly demanding. Flows in water turbines and pumps have fully developed turbulence, are constrained in curved channels of complex geometry and exhibit large downstream pressure gradients and high shear. In addition, commonly used grids have some properties usually not supported in general-purpose visualization packages, such as multi-block structured grids, rotational symmetry and zones moving relative to each other (e.g. stator and runner). The machines are highly optimized, with efficiencies exceeding 93%. Industrial simulations usually solve for steady (time-averaged) solutions of the Navier-Stokes equations. Typical vortices [19] in such flows are weak, yet these vortices are of particular interest to the engineers developing these turbomachines. Extracting vortices is thus the most important step of a feature-based visualization for this task.

Existing methods for finding vortices

Various previously published methods for vortex recognition have been found of limited applicability for typical turbomachinery flows. Methods based on isosurfaces of a scalar field (namely, *vorticity magnitude* [26], *helicity* [14], *pressure* [2] or *lambda*$_2$ [9]) are usually not able to discriminate between different structures.

We therefore concentrate on vortex recognition schemes based on the extraction of *vortex core lines*, i.e. the center lines of the vortices around which the flow spirals. Methods that assume the vortex core line to be a streamline (streamlines from critical points, [5]) or a vorticity line [25] could not be successfully applied to our data. Among existing methods for vortex core extraction, we found in [16] that the ones based on local differential geometric properties of the vector field came closest to our objectives. For both the method that places vortex cores where the curl (vorticity) is parallel to the flow, and for the eigenvector method of Sujudi and Haimes ([23], [10]), we showed that they work satisfactorily in some cases, but failed in others.

In the following, we discuss the eigenvector method and present an improved method to locate vortex core lines which can handle the case of bent vortices. This method, based on higher-order derivatives, is presented in section 2. Section 3 introduces two attributes of a vortex core – its strength and quality; section 4 presents our results on some example flows. Finally, we summarize our findings and conclude with a preview of planned future work in section 5.

2 Vortex core line method

2.1 Notation and foundations

Notation

We use lower case letters in bold font for vectors and vector fields, such as $\mathbf{x}$ and $\mathbf{v}$. Upper case letters in the same font represent matrices, such as $\mathbf{M}$ and $\mathbf{J}$. In this paper, we refer to the velocity field by $\mathbf{v}$, and to the matrix of its first derivatives (the Jacobian of $\mathbf{v}$) by $\mathbf{J}$:

$$\mathbf{J}_{ij} = \frac{\partial \mathbf{v}_i}{\partial \mathbf{x}_j}. \tag{1}$$

$\mathbf{J}$ has either three real, or one real and a pair of conjugate complex eigenvalues. The latter occurs when the *discriminant* of the characteristic equation is positive,

$$\left(\frac{Q}{3} - \frac{P^2}{9}\right)^3 + \left(\frac{QP - 3R}{6} - \frac{P^3}{27}\right)^2 > 0, \tag{2}$$

where P, Q and R are the invariants of $\mathbf{J}$, in particular $P = -\text{trace}(\mathbf{J})$ and $R = -\det(\mathbf{J})$.

We also need the third-order tensor of second derivatives of $\mathbf{v}$, written as $\mathbf{T}$:

$$\mathbf{T}_{ijk} = \frac{\partial^2 \mathbf{v}_i}{\partial \mathbf{x}_j \partial \mathbf{x}_k}. \tag{3}$$

Fluid dynamics equations

From fluid dynamics, we need to introduce the *derivative following a particle* of an arbitrary function f, denoted Df/Dt, and defined as

$$\frac{Df}{Dt} = \frac{\partial f}{\partial t} + \frac{\partial f}{\partial \mathbf{x}_1}\mathbf{v}_1 + \frac{\partial f}{\partial \mathbf{x}_2}\mathbf{v}_2 + \frac{\partial f}{\partial \mathbf{x}_3}\mathbf{v}_3. \tag{4}$$

In the remainder of the paper, we assume the vector field to be *steady*, therefore $\partial f/\partial t$ is zero. We can thus write Df/Dt using vector calculus for steady vector fields as

$$\frac{Df}{Dt} = \text{grad}\, f \cdot \mathbf{v}. \tag{5}$$

In particular, we can apply this derivative to the velocity vector itself, resulting in the *acceleration* of a particle (in steady flows):

$$\mathbf{a} = \frac{D\mathbf{v}}{Dt} = \text{grad}\,\mathbf{v} \cdot \mathbf{v} = \mathbf{J} \cdot \mathbf{v}. \tag{6}$$

This expression appears in both Euler and Navier-Stokes equations.

Differential geometry equations

From differential geometry, we will use curvature and torsion of parametric curves in R^3 given in the form

$$\mathbf{x} = \mathbf{x}(t). \tag{7}$$

With $\mathbf{x}'$, $\mathbf{x}''$ and $\mathbf{x}'''$ denoting $d\mathbf{x}/dt$, $d^2\mathbf{x}/dt^2$ and $d^3\mathbf{x}/dt^3$, respectively, we can define a *curvature vector* of $\mathbf{x}$ as

$$\mathbf{c} = \frac{\mathbf{x}' \times \mathbf{x}''}{|\mathbf{x}'|^3} \tag{8}$$

and write the curvature κ of $\mathbf{x}$ as

$$\kappa = |\mathbf{c}|. \tag{9}$$

Similarly, the *torsion* τ of $\mathbf{x}$ can be expressed as

$$\tau = \frac{(\mathbf{x}' \times \mathbf{x}'') \cdot \mathbf{x}'''}{|\mathbf{x}' \times \mathbf{x}''|^2}. \tag{10}$$

Finally, we will always assume the vector field $\mathbf{v}$ to be *nondegenerate*, that is, the vector and its derivatives up to second order are well-defined and non-zero except at isolated points.

2.2 Eigenvector method of Sujudi and Haimes

Definition

In their original publication [23], Sujudi and Haimes defined the vortex core line as the set of places where what they call the *reduced velocity* is zero. Reduced velocity is defined as the velocity minus its component in the direction of the real eigenvector of the Jacobian $\mathbf{J}$ (Eq. 1). Only regions having complex eigenvalues (Eq. 2) are considered, so there is always a single real eigenvalue and the corresponding eigenvector direction is unique. In a case study [10] this method was applied to several large data sets.

Observations

A reduced velocity of zero means that at these points, the velocity vector is parallel to the real eigenvector of $\mathbf{J}$. Equivalently, $\mathbf{v}$ *itself* is an eigenvector of $\mathbf{J}$, hence a solution of $\mathbf{J}\mathbf{v} = \lambda\mathbf{v}$.

For the assumed case of steady flow, $\mathbf{J}\mathbf{v}$ (Eq. 6) is the acceleration vector $\mathbf{a}$ of the particle. The method can thus be implemented by evaluating $\mathbf{a}$ and checking for parallel $\mathbf{v}$ without explicitly solving an eigenvalue problem.

Curvature of a vector field

Curvature of a vector field can be defined at every (nondegenerate) point by calculating the curvature of the *streamline* $\mathbf{x}(t)$. For a streamline, we have

$$\mathbf{x}' = \mathbf{v} \tag{11}$$

and, using (Eq. 6),

$$\mathbf{x}'' = \frac{D\mathbf{v}}{Dt} = \mathbf{J}\mathbf{v} = \mathbf{a}. \tag{12}$$

Therefore, the curvature vector (Eq. 8) of a vector field $\mathbf{v}$ can be calculated at any (nondegenerate) point by

$$\mathbf{c} = \frac{\mathbf{v} \times \mathbf{a}}{|\mathbf{v}|^3}, \tag{13}$$

which becomes zero if, and only if, $\mathbf{v}$ is parallel to $\mathbf{a}$ – exactly the core line according to the eigenvector method. An intuitive explanation is that a particle at this core is currently moving in direction of $\mathbf{v}$, and its acceleration $\mathbf{a}$ is parallel to $\mathbf{v}$, so it will momentarily stay on a straight line.

Another equivalent formulation of the "$\mathbf{v}$ parallel $\mathbf{a}$" condition is thus *zero curvature*. Again, (Eq. 2) is required a priori.

Optimality in globally linear vector fields

Linear vector fields, e.g. local linearizations given by a Taylor expansion, can be classified into basic patterns named sink, source, saddle, spiral sink, spiral source and spiral saddle, according to [1]. This classification can be based on the three invariants of the Jacobian, as explained in [15].

As a first test for any vortex core finder, we can therefore examine all classes of globally linear vector fields. For linear fields, the spiral patterns (also called foci) obviously do contain a vortex, and the core line is a straight streamline through the critical point of the vector field - each nondegenerate linear vector field has exactly one critical point. The other classes (sinks, sources, saddles) do not contain a vortex. The eigenvector method agrees with all cases of globally linear vector fields, which makes it superior to the other methods examined.

Problems of the eigenvector method

While the eigenvector method is correct for all purely linear vector fields, it has problems with vortices that are curved. Especially for our turbomachinery data sets, the vortex core lines found were not as expected. We showed in [16] that the method introduces an error as soon as the vortex is bent. The error increases with decreasing ratio between rate of rotation around the core and rate of rotation generated by curvature along the core. For very strong vortices or almost straight ones, the eigenvector method succeeds. Problems are caused by weakly rotating vortices with nonnegligible curvature.

These difficulties originate from the fact that using a linear vector field (the local linearization), it is not possible to model a curved vortex; linear fields can only model a straight vortex, with a straight streamline as its core line.

2.3   A higher-order method for vortex core lines

Second-order derivatives

In order to improve the definition for vortex core lines with respect to curved vortices, one obviously has to take into account higher-order derivatives in some way. We therefore introduced the tensor of second derivatives, T (Eq. 3) and use it to calculate the second derivative of v. We do this by applying the D/Dt operator (Eq. 5) to a defined in (Eq. 6). We denote this *second derivative following a particle* by b:

$$b = \frac{D^2 v}{Dt^2} = \frac{Da}{Dt} = \frac{D(Jv)}{Dt} = JJv + Tvv. \qquad (14)$$

Analogous to (Eq. 11) and (Eq. 12), this is the third derivative of a streamline $x(t)$:

$$x''' = b = JJv + Tvv. \qquad (15)$$

Zero torsion (streamline locally planar)

Similar to the curvature in (Eq. 13), the torsion (Eq. 10) of a vector field v can be written as

$$\tau = \frac{(v \times a) \cdot b}{|v \times a|^2}. \qquad (16)$$

A streamline is *locally planar* if v, a and b are coplanar, i.e. if the numerator of τ is zero:

$$(v \times a) \cdot b = 0. \qquad (17)$$

This is true even where τ is undefined because v is parallel to a.

Model of a bent vortex

The eigenvector method is based on a straight-line model for the vortex core. The core line actually generated by this method can deviate to some extent from a straight line. However, if the deviation is too large, the result is inconsistent with the underlying model.
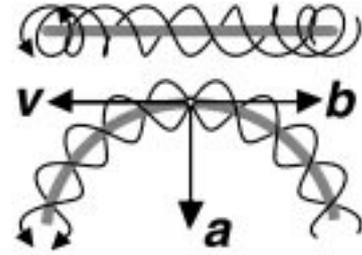
Figure 1: Front and top view of situation at core of bent helical vortex. At the core, b is antiparallel to v; a is perpendicular.

Instead, we use a curved vortex model, namely the bent helical flow introduced in [16]. In its standard form, this synthetic vortical flow has a core in the shape of a circle and acceleration on the core has a centripetal component only, as depicted in Fig. 1. This flow field is defined by

$$v_{\text{bent vortex model}} = \left(-\frac{\gamma y}{r} - \frac{\omega z x}{r^2}, \frac{\gamma x}{r} - \frac{\omega z y}{r^2}, \omega\left(1 - \frac{R}{r}\right) \right), \qquad (18)$$
$$\text{where} \qquad r = \sqrt{x^2 + y^2}$$

and conserves mass in an incompressible medium (zero divergence). Modifications of this bent vortex might consist of distorting the circular core or adding tangential acceleration.

Adapting the method for bent vortices

In order to allow curved vortex cores, the zero-curvature condition must be relaxed to a zero-torsion condition, (Eq. 17). The vortex core is a planar curve in the model (Eq. 18), but in analogy to the eigenvector method, we do not assume this property to be true for the resulting core lines in general flows.

In contrast to the zero-curvature condition, the zero-torsion condition is true on a 2D manifold, namely the zero isosurface of torsion. Therefore, a second condition is needed to restrict the solution to lines.

A possible second condition could be that zero torsion is preserved as well as possible when following the streamline. This would lead to a definition for the vortex core to be the places where torsion and its first derivative $D\tau/Dt$ are zero. This indicates that the streamline not only has a point of zero torsion at the core, but at the same time, it is tangential to the zero torsion isosurface.

The advantage of this hypothetical method is that it correctly handles the bent vortex model under a wide range of modifications. However, calculating the derivative of torsion $D\tau/Dt$ requires yet another derivative, the *third* derivative of the vector field **v**. Calculating high derivatives numerically in a discrete grid is by nature unstable and inaccurate. In practice, $D\tau/Dt = 0$ as a second condition appears too difficult to evaluate with sufficient accuracy for the resulting vortex cores to be useful: the large relative errors on a third derivative lead to excessive noise.

A numerically feasible method must avoid third derivatives of the velocity. Knowing that **b** is restricted to the $<$**v**, **a**$>$ plane by the condition of zero torsion (Eq. 17), we can now add a second condition by prescribing to **b** a fixed direction in the $<$**v**, **a**$>$ plane. Here, the best choice is to require that **b** is parallel to **v**, since this correctly describes the standard case of the bent vortex model shown in Fig. 1.

If the model is modified by adding tangential acceleration or some distortions to the circular core, solving for **b** parallel to **v** yields a core line which deviates from the actual core. However, around the core, **b** varies in direction fast enough to make these deviations small under realistic conditions. We demonstrate below that our bent helical flow can model the characteristics of vortices actually present in real CFD data.

Higher-order method for vortex cores

Based on the above motivation and supported by practical data, we suggest the following improved definition for a vortex core: *the core line is the location of all points where **b** is parallel to **v**.* This can be written as

$$\exists k, \quad \boldsymbol{JJv} + \boldsymbol{Tvv} = k\boldsymbol{v}. \tag{19}$$

Note that this vector equation represents three scalar equations for x,y,z and a new variable k; nondegenerate solutions are therefore one-dimensional.

Application to direction fields

It is possible to define a variation of our method such that vortices are determined by the *geometry* of the streamlines alone, and do not depend on the speed along these lines. This is equivalent to claiming that vortex cores should only depend on the directional information in the vector field, and not on the magnitudes of the flow vectors.

To modify the core line condition according to this requirement, one has to take the derivatives along the streamline *with respect to arc length*, as opposed to a temporal derivative. This can be achieved by *normalization* of the vectors prior to the application of the **b** parallel **v** method. This variant with prior normalization of the vector field defines the vortex core at the places where streamlines are locally circular, i.e. are planar (zero torsion) and have currently no change in curvature.

The two variants pick slightly different locations for the vortex core lines; they agree if the acceleration along the core is negligible.

2.4 Implementation Issues

Our current implementation consists of two parts: first, the vector field **b** is calculated at all gridpoint locations. Then, the problem of finding the places where **b** is parallel to **v** is solved.

Derivatives

The calculation of **b** requires second derivatives. This is currently done by implementing a D/Dt operator (Eq. 5) which calculates one derivative (Jacobian) and multiplies it by **v**. This function is then applied twice to the velocity vector **v** itself.

To calculate derivatives in a discrete grid we take all neighbor points of a vertex (26 neighbors in a structured grid) and find the linear function that fits best with respect to a least-squares criterion. This can be solved with a simple 3 by 3 matrix inversion.

As no smoothing is done within the derivative algorithm, it is advisable to use some smoothing on the data as a preprocessing step. This avoids excessive fluctuations of the calculated derivative due to discretization errors. In the near future, we plan to examine how different smoothing functions improve the numerical accuracy of the derivatives and the resulting core lines. However, images in the paper and the accompanying video have been calculated without smoothing the vector field.

Finding parallel vectors using Newton iteration

The second step consists of finding the places where two given vector fields are parallel. Our algorithm looks at all internal faces (quads or triangles) of grid cells and finds the points where the solution curve intersects the face. We have two ways to find intersection of the solution curve with a face, given the two vector fields in the corners of the face.

The first method uses Newton iteration. Starting in the center of each face, a succession of 2D Newton steps within the face approaches the solution. If the solution converges but lies outside the current face, it is discarded. This method can handle vector fields defined on the cell face by an arbitrary interpolation function, for example, a bilinear interpolation on quadrilaterals.

Analytic solution for parallel vectors

The second method calculates the analytic solution, but assumes linear interpolation on the face. Quadrilateral faces thus have to be subdivided into triangles. The search for points where two linear vector fields **g** and **h** are parallel can be reduced to an eigenvector problem in the following way: On a triangular face, a linear vector field **g** can be written as a function of local triangle coordinates u, v:

$$\boldsymbol{g} = \boldsymbol{G} \begin{bmatrix} 1 \\ u \\ v \end{bmatrix}. \tag{20}$$

Two fields are parallel when

$$\boldsymbol{G} \begin{bmatrix} 1 \\ u \\ v \end{bmatrix} = k\boldsymbol{H} \begin{bmatrix} 1 \\ u \\ v \end{bmatrix}. \tag{21}$$

If H is invertible, multiplying this by its inverse, H^{-1}, leads to

$$H^{-1} G \begin{bmatrix} 1 \\ u \\ v \end{bmatrix} = k \begin{bmatrix} 1 \\ u \\ v \end{bmatrix}, \tag{22}$$

which is an eigenvector problem $Mx = \lambda x$ with $M = H^{-1} G$. If H is not invertible but G is, then the roles of g and h can simply be swapped. If both are not invertible, no isolated solutions exist. Points where two linear vector fields are parallel on a triangle can thus be found analytically by calculating eigenvectors of a 3 by 3 matrix M.

Fig. 5 and 6 show the raw output of this algorithm: all points on a grid cell face where v is parallel to a, or b, respectively.

3 Vortex strength and quality

Both the eigenvector method and our method produce many solution points that, upon close inspection, can not be considered vortex cores, for example because there is no significant rotation present (raw points shown in Fig. 5 and 6). Therefore, besides the *location* of vortex cores discussed so far in this paper, it is also necessary to define some *attributes* on these core lines. The most important one is a measure for the strength of the vortex.

Strength of rotation

The eigenvector method assumes that some swirl is present whenever there are complex eigenvalues of the Jacobian (Eq. 2). The strength of the swirling motion is measured by the absolute value of the imaginary part of the complex eigenvalues. In our method, we prefer to do this calculation in two dimensions. Therefore, we first project the linearized vector field onto a plane perpendicular to the core velocity. The 2D discriminant is then computed, and in case of complex eigenvalues, the imaginary part is used as the measure for rotation strength.

We also determine the sign (right- or lefthanded rotation) by computing the sign of the curl of the projected flow and comparing with the local flow direction.

Quality of solution

The equations for both the eigenvector method and our method can have solution lines at a large angle to the flow vector. This does not correspond with the intuitive model of a vortex, where the core line is close to a streamline. From the set of detected vortex cores, we therefore want to eliminate lines that consistently exhibit a large angle to the flow.

We measure quality by the cosine of the angle between the vortex core and the velocity vector. For actual vortices, this angle is expected to be small.

Noise suppression

Especially in regions where there is only a slight rotation present, very short segments of vortex cores with weak rotation are found. Small and weak features are undesired, as they may stem from numerical errors (in the calculation of core lines, or in the original flow simulation). The user can therefore impose limits on minimal strength and quality in order to filter desired solutions from noise. Instead of this absolute threshold, we plan to apply a hysteresis threshold technique to the vortex core lines.

4 Preliminary results

We applied the b parallel v method to several data sets, including the two data sets used in the video accompanying [16]. Many vortical structures can be recognized by both the eigenvector and our higher-order method, but the vortex core lines often do not coincide. In such situations, the core lines produced by our method consistently exhibit better quality in the sense of the definition in section 3.
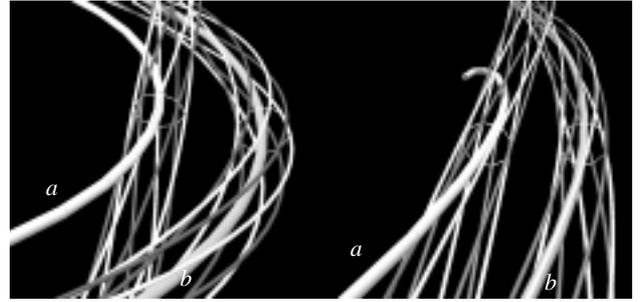
Figure 2: Comparable situation in bent vortex model (left) and practical data (right): shown are cores indicated by eigenvector (a) and b parallel v (b) methods, and a set of streamlines around each core.

Our method was designed to handle the case of the analytical flow representing a bent vortex (Fig. 2, left). Similar situations have been found in practical data sets (Fig. 2, right). As long as the flow speed along the core is uniform, the condition b parallel v holds at the vortex core. If the flow along the core accelerates however, the core line deviates from the core. For reasonable parameters, it is still closer to the actual core than the position indicated by the eigenvector method. The variant that applies normalization of the vector field prior to calculating derivatives is not disturbed by acceleration along the core. However, it can not correctly handle some distortions such as a scaling in x direction of the whole vector field. The actual vortex core of this synthetic flow field always corresponds exactly to our "hypothetical" method (zero torsion and zero derivative of torsion along a streamline), but this method is not applicable to practical data sets due to numerical instabilities in the calculation of third derivatives.

For the example field of the turbine draft tube [18], the improved method finds a vortex core that can be associated with the large swirl in this flow and also tracks the core in the curved part of the draft tube (Fig. 3). The eigenvector method detected a reasonable vortex core only in the straight end part of the data set, but none in the curved part.

For the turbine runner example data set, we selected a typical vortical structure and colored some streamlines manually to roughly indicate the structure in question (Fig. 4, top). The eigenvector method captured the start of this vortex well and tracked it to some extent; the vortex core however appeared slightly offset to the inside of the core radius (Fig. 4, bottom). This indicates that the flow in this practical data set is very consistent to our analytical model of a bent vortex. The improved method locates the core and can track it significantly further than the eigenvector method.
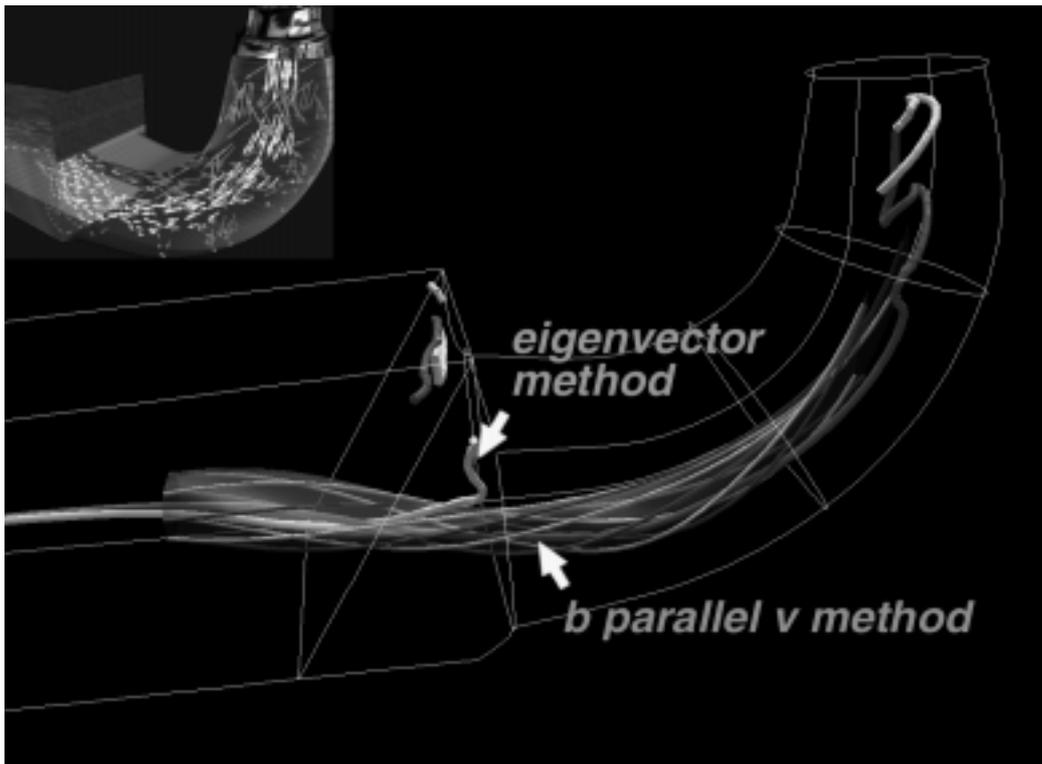
Figure 3: Vortex cores and streamlines in a water turbine draft tube.

As a final example, we applied the higher order method to the standard benchmark CFD data set, the blunt fin flow [7]. On this data set, several different vortex finding algorithms, including ours depicted in Fig. 7, agree on the location of the core line of the horseshoe vortex in front of the fin.

Our prototype implementation in AVS 5 only requires storage for the additional vector b and runs in a few minutes for typical data sets with half a million nodes.

5 Conclusions, Future Work

This paper proposes a new method to find vortex core lines. Localization of vortices has been structured into several components: To find the location of the core lines, we use the condition of b parallel v. Rotation strength is measured by projecting the linearized flow field perpendicular to the core velocity. A sign denoting the handedness of rotation is similarly computed. Finally, a quality attribute is evaluated to check for consistency.

With the test data used so far, we can conclude that the b parallel v method represents a significant improvement over the eigenvector method for flows where the curvature of vortices can not be neglected. In cases where the eigenvector method is already sufficient (due to almost straight or very strongly rotating vortices), the two methods are roughly equivalent.

Compared to the eigenvector method, our new method faces the problems of computing higher order derivatives. Careful imple-

mentation can reduce undesired "false hit" effects in the form of short, isolated vortex core segments, especially near solid boundaries.

Work is underway to extract a more symbolic description of the vortex core lines. The algorithm described here yields only a set of points (with strength and quality measurement). This is sufficient for direct display as lines, but in order to allow operations like interactive selection of vortices, the program needs a symbolic description of the line structures. Once the core lines are known, more powerful and informative visualization methods can be devised, for example by defining a vortex region around the core to depict size and shape of the whole vortex. We plan to develop such a technique in the near future and apply it to a larger set of data, mainly from the field of hydrodynamics.

Web address

`http://www.scsc.ethz.ch/SV/turbo`
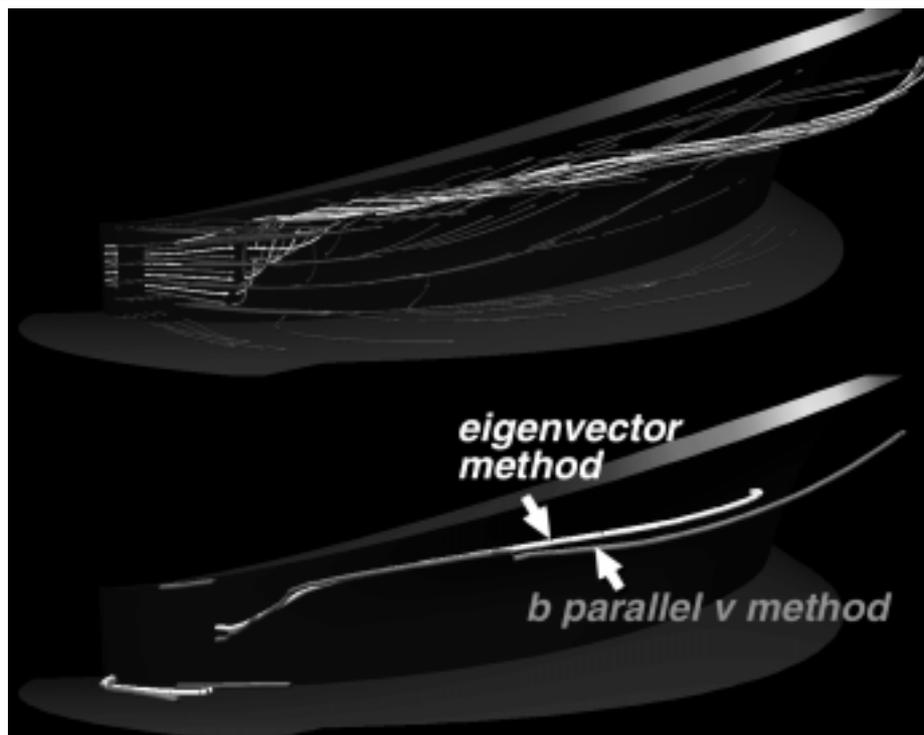
Figure 4: Streamlines (top) and core lines (bottom)in a turbine runner at part load.

References

[1]   Asimov, D.: "Notes on the Topology of Vector Fields and Flows". In *Proceedings of Visualization '93*, San Jose, 1993.

[2]   Banks, D. C. and B. A. Singer: "Vortex Tubes in Turbulent Flows: Identification, Representation, Reconstruction". In *Proceedings of IEEE Visualization '94*, Washington, DC, pp. 132–139, October 1994.

[3]   Cabral, B. and L. Leedom: "Imaging Vector Fields using Line Integral Convolution". In *Computer Graphics `93 (SIGGRAPH) Conference Proceedings*, pp. 263-270, Los Angeles, CA, August 1993.

[4]   Crawfis, R. A. and N. Max: "Texture Splats for 3D Scalar and Vector Field Visualization". In *Proceedings of Visualization '93*, pp. 261–265, October 1993.

[5]   Globus, A., C. Levit, and T. Lasinski: "A Tool for Visualizing the Topology of 3D Vector Fields". In *Proceedings of Visualization '91*, pp.33–39, San Diego, CA, October 1991.

[6]   Helman, J. L. and L. Hesselink: "Visualizing Vector Field Topology in Fluid Flows". In *IEEE Computer Graphics and Applications*, 11(3):36–46, May 1991.

[7]   Hung, C.M. and P.G. Buning: "Simulation of Blunt-Fin Induced Shock Wave and Turbulent Boundary Layer Separation". AIAA Paper 84-0457, *AIAA Aerospace Sciences Conference*, Reno, NV, January 1984.

[8]   Interrante, V. and C. Grosch: "Strategies for Effectively Visualizing 3D Flow with Volume LIC". In *Proceedings of Visualization '97*, Phoenix, AZ, pp. 421–424, October 1997.

[9]   Jeong, J. and F. Hussain: "On the identification of a vortex". In *Journal of Fluid Mech.*, 285:69–94, 1995.

[10] Kenwright, D. and R. Haimes: "Vortex Identification - Applications in Aerodynamics". In *Proceedings of Visualization '97*, Phoenix, AZ, pp. 413–416, October 1997.

[11] Krivchenko, G. I.: *Hydraulic Machines: Turbines and Pumps*. 2nd ed., ISBN 1-56670-001-9, CRC Press, 1994.

[12] Lavin, Y. and Y. Levy: "Singularities in Nonuniform Tensor Fields". In *Proceedings of Visualization '97*, Phoenix, AZ, pp. 59–66, October 1997.

[13] de Leeuw, W. and J.van Wijk: "Enhanced Spot Noise for Vector Field Visualization". In *Proceedings of Visualization '95*, Atlanta, GA, pp. 233–239, October 1995.

[14] Levy, Y, D. Degani and A. Seginer: *Graphical Visualization of Vortical Flows by Means of Helicity*. AIAA 28(8), pp. 1347–1352, August 1990.

[15] Perry, A. E. and M. S. Chong: "Topology of Flow Patterns in Vortex Motions and Turbulence". In *Eddy Structure Identification in Free Turbulent Shear Flows*, ed. J. P Bonnet and M. N. Glauser, Kluwer Academic Publishers, 1992.

[16] Roth, M. and R. Peikert: "Flow Visualization for Turbomachinery Design". In *Proceedings of IEEE Visualization '96*, San Francisco, CA, pp. 381–384, October 1996.

[17] Scheuermann, G., H. Hagen, H. Krüger, M. Menzel and A. Rockwood: "Visualization of Higher Order Singularities in Vector Fields". In *Proceedings of Visualization '97*, Phoenix, AZ, pp. 67–71, October 1997.

[18] Sebestyen, A. and H. Keck, "Uprating of Ultra-Low Head Francis Units based on Numerical Flow Analysis". In *Proceedings of Water Power Conference on Uprating and Refurbishing Hydro Powerplants*, Nice, France, 1995.

[19] Sebestyen, A. and R. Peikert: "Simulation of Turbomachinery Secondary Flow Phenomena". In *Proceedings of European Modeling and Simulation Multiconference*, pages 590-594, Panum Institute, Copenhagen, Denmark, June 1991.

[20] Silver, D. and X. Wang: "Volume Tracking". In *Proceedings of IEEE Visualization '96*, San Francisco, CA, pp. 157–164, October 1996.

[21] Sadarjoen, A., F. Post: "Deformable Surface Techniques for Field Visualization". In *Proceedings of Eurographics '97*, pp. 109–116, Budapest, September 1997.

[22] Stalling, D. and H. Hege: "Fast and Resolution Independent Line Integral Convolution". In *Computer Graphics `95 (SIGGRAPH) Conference Proceedings*, pages 249–256, Los Angeles, August 1995.

[23] Sujudi, D. and R. Haimes: *Identification of Swirling Flow in 3D Vector Fields*. Tech. Report, Dept. of Aeronautics and Astronautics, MIT, Cambridge, MA, 1995.

[24] Villasenor, J. and A. Vincent: "An Algorithm for Space Recognition and Time Tracking of Vorticity Tubes in Turbulence". In *CVGIP Image Understanding*, 55(1):27–35, January 1992.

[25] Yates, L. A. and G. T. Chapman, "Streamlines, Vorticity Lines, and Vortices". In *29th Aerospace Sciences Meeting*, Reno, NV, AIAA 91-0731, January 1991.

[26] Zabusky, N. J., O. N. Boratav, R, B. Pelz, M. Gao, D. Silver and S. P. Cooper: "Emergence of Coherent Patterns of Vortex Stretching during Reconnection: A Scattering Paradigm". In *Phys. of Fluids A* 2(5), p. 2469, 1991.
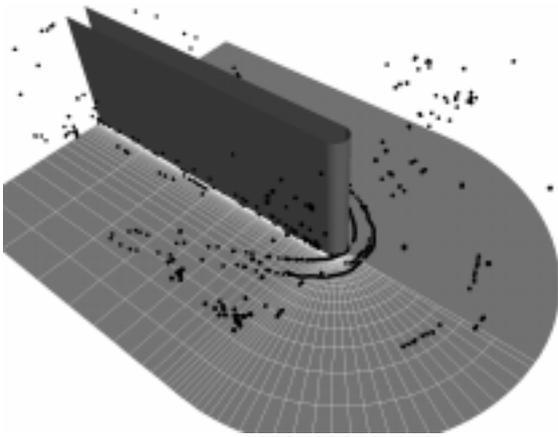
Figure 5: All points where $\mathbf{a}$ is parallel to $\mathbf{v}$ (Eigenvector method) in the blunt fin data set. The main horseshoe vortex is strong enough to be detected by the eigenvector method in spite of its curvature.
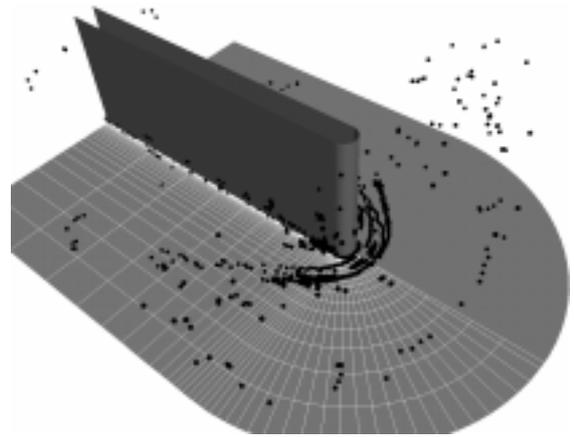
Figure 6: All points where $\mathbf{b}$ is parallel to $\mathbf{v}$. Although second-order derivatives are calculated numerically, the increase in noise in comparison to the eigenvector is tolerable.
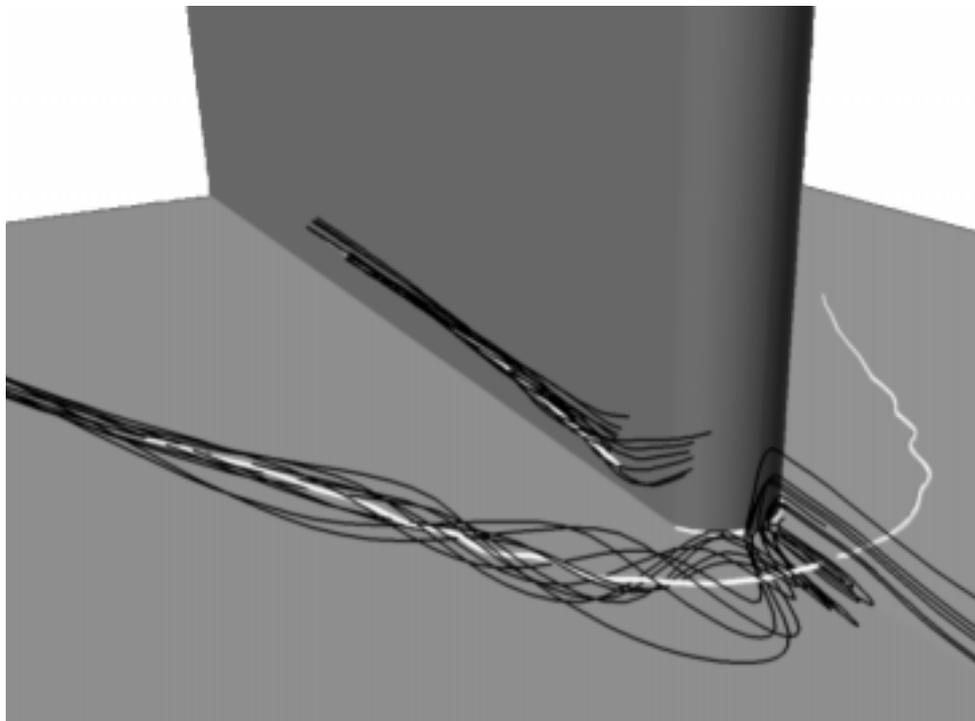
Figure 7: Core lines (white) detected by the b parallel v method, and some streamlines (black) in the blunt fin data set.
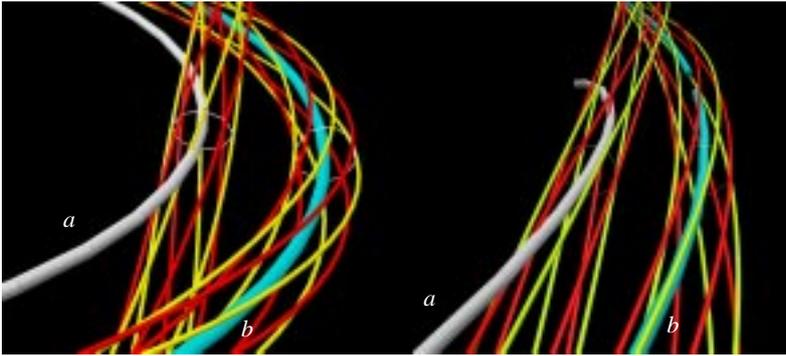
Figure 2. Comparable situation in bent vortex model (left) and practical data (right): shown are cores indicated by eigenvector (a) and b parallel v (b) methods, and a set of streamlines around each core.
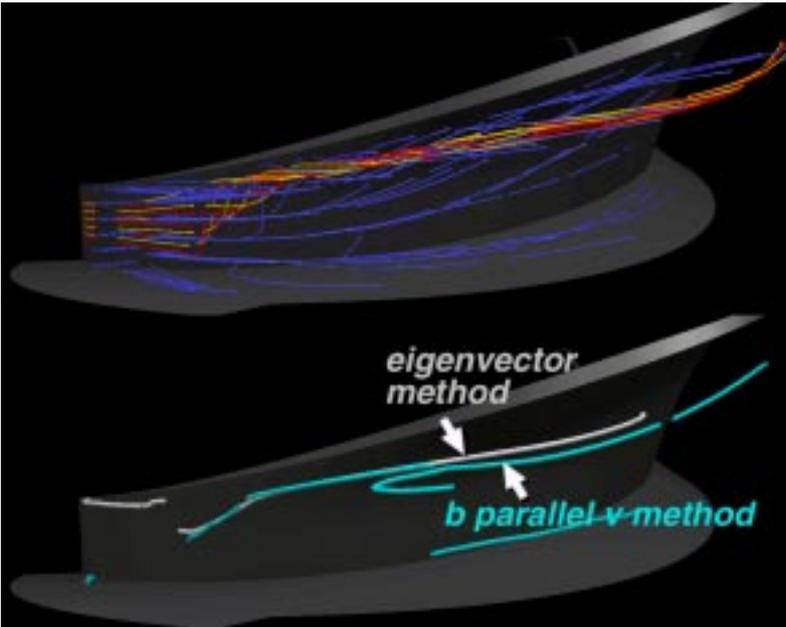
Figure 4. Streamlines (top) and core lines (bottom) in a turbine runner at part load.

Figure 3. Vortex cores and streamlines in a water turbine draft tube.